Science & Technology Development Journal 2023, 26(4):3060-3068

Open Access Full Text Article

Research Article

Effects of source correction on positron annihilation lifetime spectroscopic analysis of graft-type polymer electrolyte membranes

Nguyen Huynh My Tue[1,2], Tran Hoang Long[1,2], Dinh Tran Trong Hieu[1,2], Lam Hoang Hao[1,2], Vo Thi Kim Yen[1,2], Nguyen Manh Tuan[1,2], Huynh Truc Phuong[2,3], Le Quang Luan[4], Pham Thi Thu Hong[5], Tran Van Man[2,6], Tran Duy Tap[1,2,*]

[1]Faculty of Materials Science and Technology, University of Science, Ho Chi Minh City, 227 Nguyen Van Cu, District 5, Ho Chi Minh City, Vietnam

[2]Vietnam National University, Ho Chi Minh City, Vietnam

[3]Faculty of Physics and Engineering Physics, University of Science, Ho Chi Minh City, 227 Nguyen Van Cu, District 5, Ho Chi Minh City, Vietnam

[4]Biotechnology Center of Ho Chi Minh City, Ho Chi Minh City, Vietnam

[5]Research and Development Center for Radiation Technology (VINAGAMMA), Ho Chi Minh City, Vietnam

[6]Applied Physical Chemistry Laboratory, University of Science, Ho Chi Minh City, 227 Nguyen Van Cu, District 5, Ho Chi Minh City, Vietnam

Correspondence

Tran Duy Tap, Faculty of Materials Science and Technology, University of Science, Ho Chi Minh City, 227 Nguyen Van Cu, District 5, Ho Chi Minh City, Vietnam

Vietnam National University, Ho Chi Minh City, Vietnam

Email: tdtap@hcmus.edu.vn

History

- Received: 2023-03-05
- Accepted: 2023-11-20
- Published Online: 2023-12-31

DOI : https://doi.org/10.32508/stdj.v26i4.4052

Check for updates

ABSTRACT

Introduction: Recently, the free-volume hole features of poly(styrene sulfonic acid) (PSSA)-grafted poly(ethylene-co-tetrafluoroethylene) polymer electrolyte membranes (ETFE-PEMs) have been studied using positron annihilation lifetime spectroscopy (PALS) to determine the relationship between gas crossover through a PEM and a fuel cell. As one such series, this work investigates the source correction in PAL spectroscopic analysis for ETFE-PEM. **Method:** ETFE-PEM was prepared by radiation-induced graft polymerization and subsequent sulfonation. The free-volume hole characteristics of ETFE-PEM with a grafting degree (GD) of 106% were determined using PALS with and without source correction. **Results:** After source correction, the original-ETFE and ETFE-PEM strains exhibited increases in r_3 (smaller radius of free-volume holes in the lamellar amorphous regions, the PSSA grafts, and the interface zones inside the lamellae) and r_4 (larger radius of free-volume holes in the mobile amorphous layers and the PSSA grafts outside of the lamellae). In addition, the full width at half maximum (FWHM) of r_3 is much greater than that of r_4 due to the rearrangement in the mobile amorphous region and the polystyrene layers outside the lamellar structure. **Conclusion:** Source correction causes a significant change in the distribution curves of r_3 for the original-ETFE and ETFE-PEM. Thus, source correction of positron annihilation lifetime spectroscopic analyses is an important issue for determining the *o*-Ps lifetime of polymers, which is near the lifetime of positrons in source materials.

Key words: Positron annihilation lifetime spectroscopy, ortho-positronium, free-volume hole, polymer electrolyte membrane, fuel cell

INTRODUCTION

Proton exchange membrane fuel cells (PEMFCs) have received much attention for novel power generation because these devices result in no emission of environmental pollutants, high energy generation efficiency, low operating temperature, and quick operation[1]. PEMFCs can be applied in transportation, mobile communication equipment, charging stations, etc.[2]. Nafion is one of the most common commercial membranes used for PEMs[3–5]. However, its limitations, such as high cost and low performance at high temperature (> 100 °C) and low relative humidity (RH) (RH < 50%), have triggered the development of alternative membrane materials for PEMs. Recently, poly(styrene sulfonic acid)-grafted poly(ethylene-co-tetrafluoroethylene) (EP) electrolyte membranes (ETFE-PEMs) have been studied intensively to replace Nafion because of their competitive price, performance, and durability. Compared with Nafion, the ETFE-PEM shows greater mechanical strength, conductance, and microstructural stability under immersed conditions[6–9].

Positron annihilation lifetime spectroscopy (PALS) is a potential method that provides molecular and nanoscale information on the free-volume hole features of materials through the lifetime and annihilation intensity of positron and positronium (Ps) ions. Positronium is the metastable hydrogen-like bound state of a positron and an electron. Ps freely has two intrinsic lifetimes, namely, para-positronium (*p*-Ps, singlet state of Ps) and ortho-positronium (*o*-Ps, triplet state of Ps). In the singlet state, *p*-Ps emit two energetic photons at 511 keV with a typical lifetime of 0.125 ns in vacuum. In the triplet state, *o*-Ps has a self-annihilation lifetime of 142 ns in vacuum and emits three continuous energies from 0 to 511 keV. In essence, the lifetime of *o*-Ps (142 ns) is usually shortened to a few nanoseconds (1–10 ns) by picking up a molecular electron with an opposite spin to that of the positron (the "pick-off" mechanism)[10,11]. Recently,

Cite this article : Tue N H M, Long T H, Hieu D T T, Hao L H, Yen V T K, Tuan N M, Phuong H T, Luan L Q, Hong P T T, Man T V, Tap T D. **Effects of source correction on positron annihilation lifetime spectroscopic analysis of graft-type polymer electrolyte membranes**. *Sci. Tech. Dev. J.* 2023; 26(4):3060-3068.

VNUHCM PRESS

free-volume hole features of ETFE-PEM have been probed by PALS[12–14]. The PALS of ETFE-PEM was analyzed using 4 lifetime components. The shortest lifetime, τ_1 ~ 0.125 ns, corresponds to the lifetime of the *p*-Ps, the moderate lifetime, τ_2 ~ 0.3–0.5 ns, is the lifetime of the free positron, and the longer lifetimes, τ_3 and τ_4, are attributed to the lifetime of the *o*-Ps. The obtained results predicted that gas molecules pass more dominantly through the mobile amorphous zones and the PSSA grafts outside of the lamellae than through the inside. Moreover, the free-volume hole size of the ETFE-PEM is lower than that of Nafion, leading to less gas passing through the membrane. However, the above studies did not address in detail the effect of source correction in positron annihilation lifetime spectroscopic analysis, although this issue is quite important, as reported previously[15–18]. Therefore, this work studies the effect of source correction on the PAL spectroscopic analysis of ETFE-PEM.

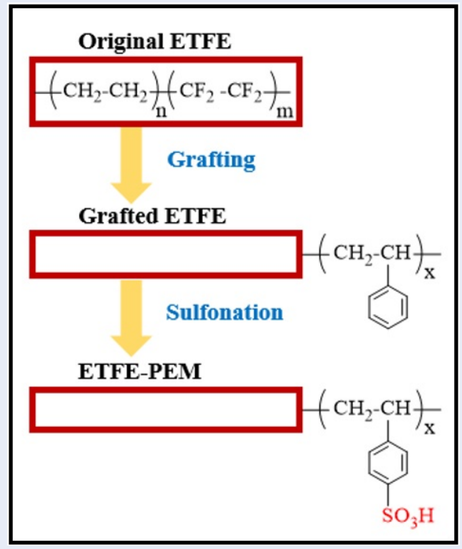

Figure 1: **Synthetic scheme and molecular structures of ETFE-PEM obtained via radiation-induced graft polymerization of styrene onto an ETFE substrate to obtain the grafted-ETFE film and subsequent sulfonation**.

EXPERLMENTAL

Materials and preparation

Figure 1 shows that the preparation process of ETFE-PEM consists of two main steps: graft polymerization and sulfonation. Commercial ETFE films were obtained from Asahi Glass Co. Ltd., Tokyo, Japan, and had the same thickness of 50 μm. The ETFE films were irradiated by gamma rays from a ^{60}Co source with an absorbed dose of 15 kGy under an argon atmosphere. The irradiated samples were immersed immediately in a styrene solution of toluene at 60 °C for 24 h for graft polymerization. These obtained films were subsequently immersed in a toluene solution at 50 °C for 24 h to eliminate the homopolymers and the residual monomers. Then, a polystyrene-grafted ETFE film (grafted-ETFE) was obtained. The grafting degree (GD) was determined by the formula GD (%) = 100(Wg – Wo)/Wo, where Wo and Wg are the weights of the film before and after graft polymerization, respectively. The grafted-ETFE was then sulfonated with chlorosulfonic acid in 1,2-dichloroethane at 50 °C for 6 hours. The membrane was washed again with pure water at 50 °C for 24 h to obtain ETFE-PEM[19,20]. In this study, grafted-ETFEs and ETFE-PEMs with a GD of 106% were utilized for positron annihilation lifetime spectroscopic analysis. This GD was selected because the graft layers are high enough to clearly investigate the effects of source correction.

PALS measurement

PALS measurements were performed using a ^{22}NaCl (20 μCi) positron source at room temperature under vacuum. Several pieces of identical samples were cut into 1x1.5 cm^2 pieces and stacked with a total thickness of 1 mm to ensure that all annihilation events occurred within the samples. Before conducting the PALS measurements, the ETFE-PEM was dried in a vacuum oven at 40 °C for 24 h to remove water molecules. **Figure 2** shows the function and operation of a photon–photon delay random coincidence spectrometer for lifetime detection[21,22]. When a positron (E_{max} = 0.54 MeV) is emitted from a ^{22}NaCl source, a high-energy gamma-ray of 1.274 MeV is produced simultaneously and marked as the start signal of the positron. The positron penetrates, heats, and diffuses in the sample and then annihilates with an electron to provide annihilation photons (stop signal). The time difference between the start and stop signals is specified as the positron or positronium lifetime. In this study, source correction was carried out at 372 ps with a 10% annihilation intensity[23]. The PAL spectrum was combined into (1–3)x10^6 counts or more to ensure statistical support for subsequent analyses. The analysis was performed by using LT v9 software[24].

PALS analysis

In this study, the subnanometer holes in all the samples are assumed to be spherical. This assumption is used for many PAL spectroscopic analyses of polymers[13]. The relationship between the hole radius and

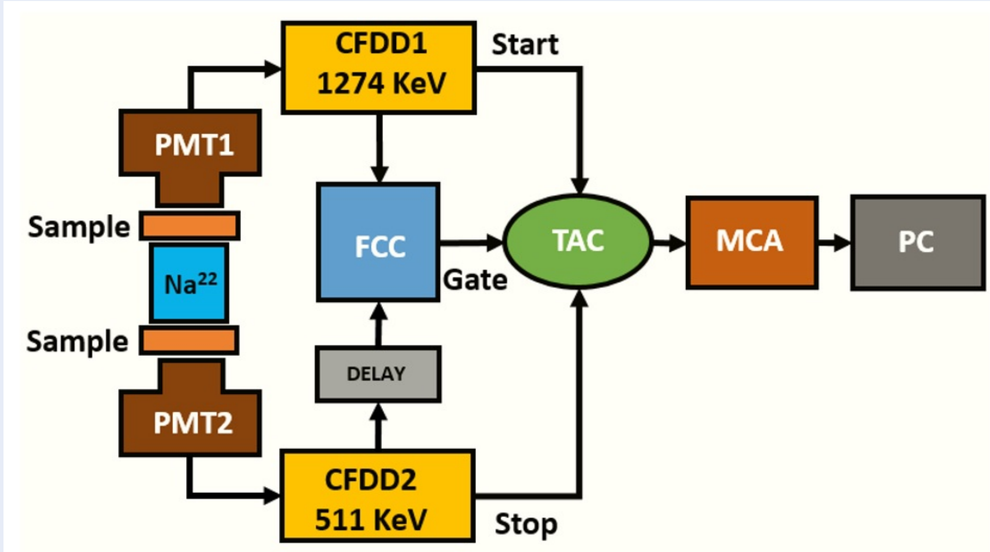

Figure 2: **Experimental diagram for the PALS measurements. The setup included a photomultiplier tube (PMT), a constant–fraction differential discriminator (CFDD), a fast coincidence unit (FCC), a time–to–amplitude converter (TAC), a multichannel analyzer (MCA), and a computer (PC)**.

the lifetime of ortho-positronium trapped in the holes is shown by the Tao–Eldrup (TE) model, which is represented by the following formula[10,25]:

$$\tau_i = \frac{1}{2}\left[1 - \frac{r_i}{r_i + \triangle r} + \frac{1}{2\pi}\sin\left(\frac{2\pi r_i}{r_i + \triangle r}\right)\right]^{-1} \quad (1)$$

where τ_i (ns) (i = 3, 4) is the lifetime component, r_i is the pore radius (nm), and ΔR ($\approx$ 0.166 nm) is the thickness of the electron layer.

The nanohole volume, V_i, is determined by the equation [10,25]:

$$V_i = \frac{4}{3}\pi r_i^3 \quad (2)$$

In addition, the radius distribution provides important information about the distribution features calculated based on the following equation[24,26]:

$$n(r) = -2\triangle r\left[\frac{2\pi r_i}{r_i + \triangle r} - 1\right]\frac{\alpha_i(\lambda)}{(r_i + \triangle r)^2} \quad (3)$$

where $\alpha_i\,(\lambda)$ is the probability density function of the o-Ps annihilation rate (λ_{io}) defined through the following formula:

$$\alpha_i(\lambda)\lambda d\lambda = \frac{1}{\sigma_i^*(2\pi)^{1/2}} \times exp\left[-\frac{(\ln\lambda - \ln\lambda_{io})^2}{2(\sigma_i^*)^2}\right]d\lambda \quad (4)$$

where λ_{io} is the maximum position of $\alpha_i(\lambda)\lambda$ and $\sigma_i^* = \sigma_1(\lambda)$ is the standard deviation quantity of the i-th distribution.

The pore volume distribution is also estimated using the following equation:

$$g(V_i) = n(r_i)/4\pi r_i^3 \quad (5)$$

RESULTS

Figure 3 shows typical decay curves of positron annihilation in the original ETFE, grafted-ETFE, and ETFE-PEM with a GD of 106%. The PALS of the original ETFE plot shows at least two slopes with a decrease at approximately 2 ns. The decay curves of grafted-ETFE and ETFE-PEM differ from each other and from that of pristine ETFE. Based on the decay curve features, the spectra of all the samples were analyzed using a four-component model, as shown in **Table 1**.

Table 1 shows the positron lifetime (τ_i) and intensity (I_i) (i = 1–4) for the original ETFE, grafted-ETFE, and ETFE-PEM at a GD of 106% with and without source correction. For the pristine ETFE, the first component (τ_1 = 0.170 ns) is attributed to the mean lifetimes of para-positronium and free positrons in the crystalline lamellar region[27,28]. The value of τ_1 is not significantly changed by the source correction (0.174 ns). The second lifetime component (τ_2 = 0.441 ns) is assumed to be the mean lifetime of the free positron in the amorphous phases[27]. The value of τ_2 (0.463 ns after source correction) is near the correction value of the source material (0.372 ns), so it significantly

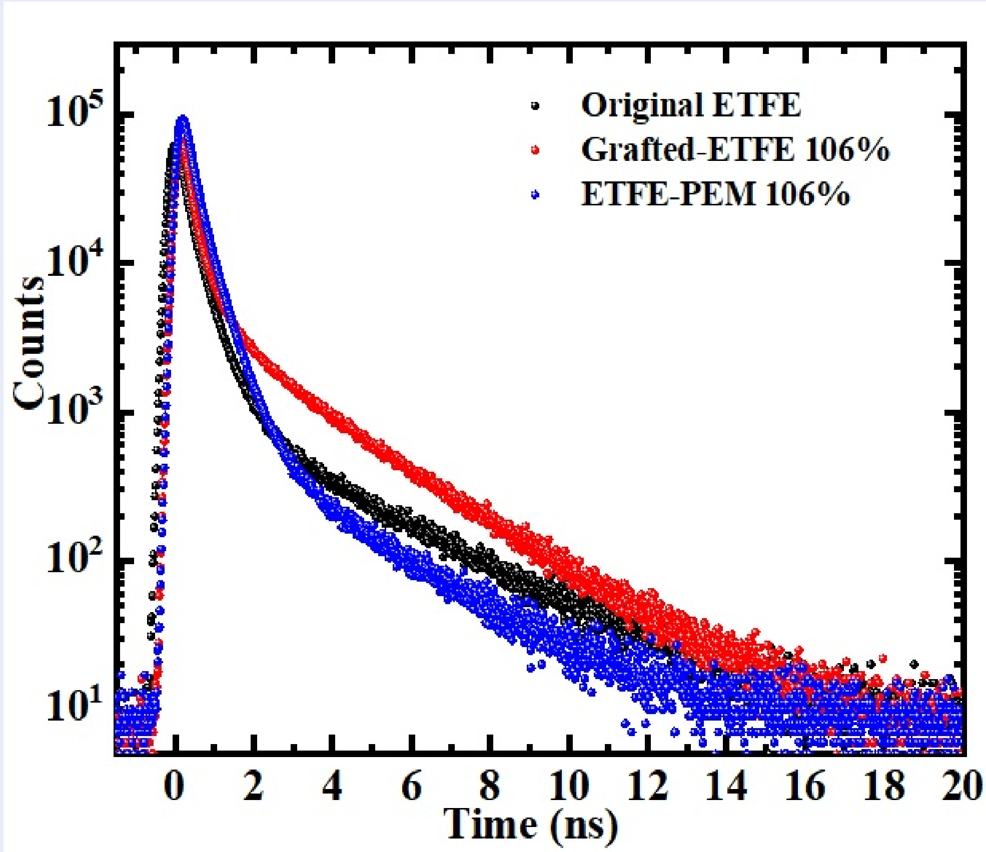

Figure 3: **PAL spectra of the pristine ETFE, grafted-ETFE, and ETFE-PEM samples with a GD of 106%**.

changes. The longer lifetimes (τ_3 = 1.620 ns and τ_4 = 3.556 ns) are attributed to the annihilation of *o*-Ps in the free-volume voids in the amorphous lamellar and interfacial regions (τ_3) and the mobile amorphous region (τ_4), respectively[12]. Like for τ_2, for τ_3 (1.790 ns after source correction), the value is close to the correction value of the source material, so the change is more significant than that for τ_4 (3.610 ns). For the grafted-ETFE film, the values of τ_1 and τ_2 are similar to those of the original ETFE film. However, τ_3 is assigned to the mean lifetime of *o*-Ps in different amorphous phases within the lamella, and τ_4 is assigned to the mean lifetime of *o*-Ps in mobile amorphous phases and polystyrene layers outside of the lamella[27,28].

Figure 4 shows the distribution curves of hole radii a) r_3 and b) r_4 for the original ETFE, grafted-ETFE, and ETFE-PEM with source correction (solid line) and without source correction (break line). As shown in **Figure 4**a, the hole radius r_3 of the original ETFE is quite symmetrical, and the radius distribution peak is shifted to a higher position by source correction. Moreover, the distribution curve of the grafted-ETFEs shows symmetry and no change in peak position. For the ETFE-PEM, the curve features are similar to those of the original ETFE, the two peaks are more separated, and the peak is shifted to a higher position after source correction. In **Figure 4**b, the hole radius distribution r_4 for the original ETFE is similar to that of r_3. In the grafted-ETFE and ETFE-PEM samples, two peaks show symmetry and no change in peak position.

Figure 5 shows the free hole volume distribution curves of a) V_3 and b) V_4 for the original ETFE, grafted-ETFE, and ETFE-PEM without (solid line) and with source correction (break line). As shown in **Figure 5**a, the distribution curves of both the original ETFE and ETFE-PEM products show partially separated peaks, no symmetry with the presence of tails, and peak positions that shift to higher values after source correction. In contrast, the distribution curve of grafted-ETFEs is quite symmetrical with a small tail and shows little change in peak position. **Figure 5**b shows more symmetry in the distribution curves of V_4 for all the samples, but the peak position shifted to

Table 1: Results of the PAL spectroscopic analyses with and without source correction for the original ETFE, grafted-ETFE, and ETFE-PEM with a GD of 106%

Samples	τ_1 (ns)	τ_2 (ns)	τ_3 (ns)	τ_4 (ns)	I_1 (%)	I_2 (%)	I_3 (%)	I_4 (%)
Without source correction								
Original ETFE	0.170 ± 0.009	0.441 ± 0.007	1.620 ± 0.190	3.556 ± 0.082	37.4 ± 1.9	51.7 ± 1.9	3.8 ± 0.4	7.1 ± 0.6
Grafted-ETFE 106%	0.175 ± 0.006	0.435 ± 0.022	1.720 ± 0.150	2.893 ± 0.079	43.6 ± 1.9	26.6 ± 1.5	12.6 ± 1.7	17.2 ± 2.0
ETFE-PEM 106%	0.168 ± 0.007	0.432 ± 0.008	1.074 ± 0.097	2.436 ± 0.048	33.2 ± 1.1	57.0 ± 1.0	4.5 ± 0.6	5.5 ± 0.3
With source correction								
Original ETFE	0.174 ± 0.006	0.463 ± 0.008	1.790 ± 0.230	3.610 ± 0.110	39.4 ± 0.9	48.4 ± 0.9	4.4 ± 0.6	7.8 ± 0.8
Grafted-ETFE 106%	0.168 ± 0.005	0.460 ± 0.025	1.720 ± 0.150	2.894 ± 0.079	45.5 ± 1.8	21.4 ± 1.1	13.9 ± 1.8	19.2 ± 2.1
ETFE-PEM 106%	0.176 ± 0.004	0.454 ± 0.006	1.270 ± 0.150	2.444 ± 0.039	36.4 ± 0.6	53.8 ± 0.5	4.0 ± 0.2	5.8 ± 0.4

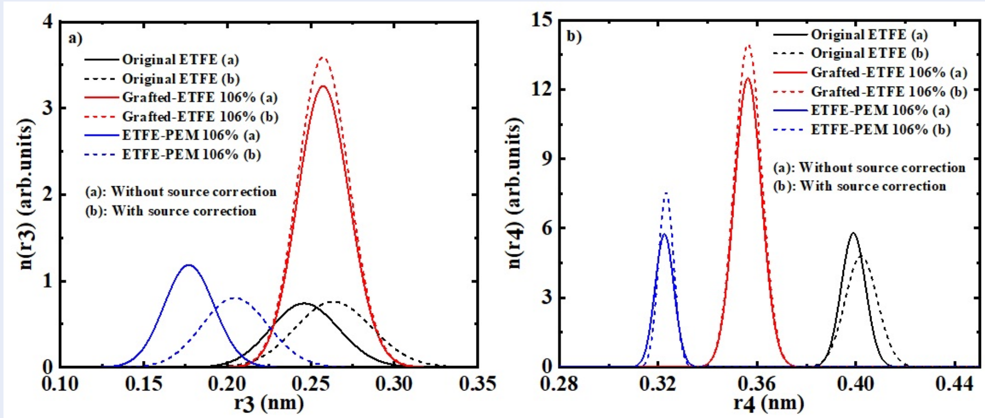

Figure 4: **Hole radius distributions (r_3 and r_4) of the original ETFE, grafted-ETFE, and ETFE-PEM with a GD of 106% with and without source correction**.

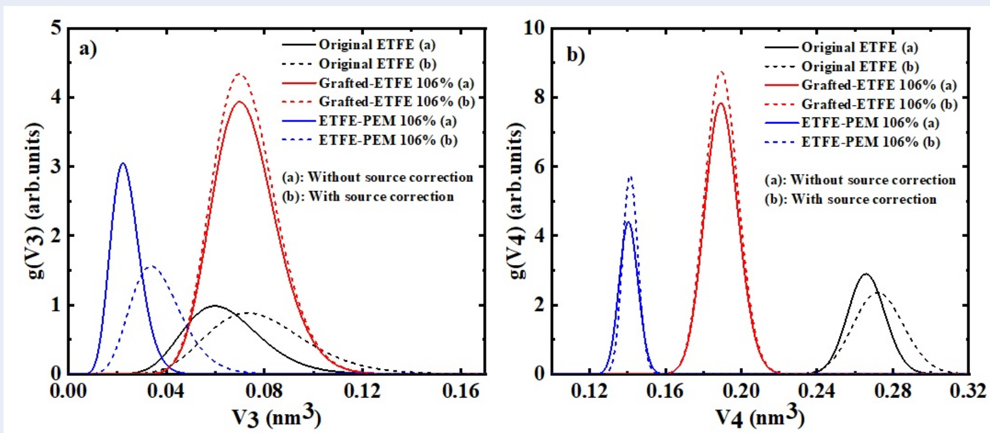

Figure 5: **Hole volume distributions (V_3 and V_4) in the original ETFE, grafted-ETFE, and ETFE-PEM with a GD of 106% with and without source correction**.

a higher value after source correction was applied for the pristine ETFE sample.

DISCUSSION

The lifetime and annihilation intensity parameters before and after source correction are shown in **Table 1**. It is clear that τ_3 and τ_4 of grafted-ETFE do not show the effect of the source correction. In contrast to those of the grafted-ETFE, the lifetime of the ETFE-PEM significantly changes in response to source correction, in which τ_3 and τ_4 increase from 1.074 and 2.436 to 1.270 and 2.444 ns, respectively. The annihilation intensities I_1, I_3, and I_4 increase in all three samples, while I_2 decreases after source correction. The results of the distribution curve (**Figure 4**a) show that the source correction has an effect on the size of the free hole radius in the amorphous lamellar region, most clearly in the original ETFE and ETFE-PEM. Like in **Figure 4**b, according to the obtained results, the hole radius in amorphous lamellae but not in mobile amorphous phases or polystyrene layers outside the lamellar regions is strongly affected by source correction.

Table 2 shows the r_3, r_4, FWHM(r_3), and FWHM(r_4) values for the original ETFE, grafted-ETFE, and ETFE-PEM without and with source correction. The pore sizes r_3 and r_4 obtained from the distribution curves are consistent with those calculated using the Tao–Eldrup equation. The FWHM(r_3) and FWHM(r_4) values of the original ETFE and ETFE-PEM increase after source correction, which is similar to the changes in the corresponding r_3 and $r_{4\ values}$. Moreover, the FWHM(r_4) is much lower than the FWHM(r_3). The result can be elucidated from the fact that the amorphous lamellar region is stiffer and less mobile than mobile amorphous phases and polystyrene layers outside of the lamellar structure, which can be rearranged, resulting in a smaller FWHM(r_4)[12,13]. **Table 3** presents the V_3, V_4, FWHM(V_3), and FWHM(V_4) values. The hole volume distributions of V_3 and V_4 obtained from the distribution curves are also in agreement with those calculated using the Tao–Eldrup equation. The FWHM(V_3) and FWHM(V_4) values of the original ETFE and ETFE-PEM increase after the source correction, which is similar to the changes in the corresponding V_3 and V_4. Moreover, the FWHM(V_4) is much lower than the FWHM(V_3), which is similar to the FWHM(r_3) and FWHM(r_4) values, as shown in **Table 2**. Thus, the same mechanism can be proposed for this result.

CONCLUSION

Positron annihilation lifetime spectroscopic analyses were performed to observe the effect of source correction for the original ETFE, grafted-ETFE, and ETFE-PEM with a GD of 106%. r_3, r_4, FWHM (r_3), and FWHM (r_4) of the original ETFE and ETFE-PEM but not the grafted ETFE increase after source correction. Similar results are also obtained for V_3, V_4, the FWHM (V_3), and the FWHM (V_4). Interestingly, the FWHM (for r_4 and V_4) was much lower than the FWHM (for r_3 and V_3). This result indicates that the amorphous lamellar region is less mobile than the amorphous phases and polystyrene layers located outside of the lamellar structure; additionally, the amorphous lamellar region can be rearranged, leading to smaller FWHM values (r_4 and V_4). Note that source correction significantly influences the distribution curves of r_3 and V_3 of the original-ETFE and ETFE-PEM. This result suggested that source correction during positron annihilation lifetime spectroscopic analyses is an important issue for determining the *o*-Ps lifetime of polymers, which is near the lifetime of the positron in the source materials.

LIST OF ABBREVIATIONS

ETFE: Poly(ethylene-co-tetrafluoroethylene)
ETFE-PEM: Polystyrene Sulfonic Acid (PSSA)-Grafted Poly(ethylene-co-Tetrafluoroethylene) Polymer Electrolyte Membranes
FWHM: Full width at half maximum
GD: Grafting degree
grafted-ETFE: Polystyrene (PS)-Grafted Poly(ethylene-co-Tetrefluoroethylene) Polymer Electrolyte Membranes
***o*-Ps:** Ortho-Positronium
PALS: Positron Annihilation LifeTime Spectroscope
PEM: Polymer electrolyte membrane
***p*-Ps :** Para-Positronium
Ps: Positronium
PSSA: Polystyrene Sulfonic Acid
RH: Relative humidity
TE: Tao-Eldrup

AUTHOR CONTRIBUTION

Tran Duy Tap: Conceptualization, Project Administration, Fundingacquisition, Supervision, Resources, Investigation, Methodology, Data curation, Formalanlysis, Supervision, Validation, Visualization, Writing – original draft, Writing – review & editing. **Nguyen Huynh My Tue:** Investigation, Methodology, Data curation, Formalanysis, Supervision, Validation, Visualization, Writing – original draft, Writing – review & editing. **Tran Hoang Long, Dinh Tran Trong Hieu, Lam Hoang Hao, Vo Thi Kim Yen, Nguyen Manh Tuan:** Visualization, Validation, Investigation, Writing – review & editing. **Huynh Truc Phuong, Le Quang Luan, Pham Thi Thu Hong, and Tran Van Man:** Visualization, Validation, Datacuration. All authors read and approved the final manuscript.

CONFLICT OF INTEREST

The authors declare that they have no conflicts of interest.

ACKNOWLEDGMENTS

This research is funded by the Vietnam National Foundation for Science and Technology Development (NAFOSTED) under grant number 103.99-2020.59. The authors thank Dr. Luu Anh Tuyen (Center for Nuclear Techniques, Vietnam Atomic Energy Institute) for the PALS experiments.

DATA AVAILABILITY STATEMENT

The datasets are not publicly available but are available from the corresponding author upon reasonable request.

REFERENCES

1. Tanç B, Arat HT, Baltacıoğlu E, Aydın K. Overview of the next quarter century vision of hydrogen fuel cell electric vehicles. Int J Hydrogen Energy. 2019;44(20):10120-8;Available from: https://doi.org/10.1016/j.ijhydene.2018.10.112.
2. Wang Y, Ruiz Diaz DF, Chen KS, Wang Z, Adroher XC. Materials, technological status, and fundamentals of PEM fuel cells - A review. Mater Today. 2020;32(xx):178-203;Available from: https://doi.org/10.1016/j.mattod.2019.06.005.
3. Karimi MB, Mohammadi F, Hooshyari K. Recent approaches to improve Nafion performance for fuel cell applications: A review. Int J Hydrogen Energy. 2019;44(54):28919-38;Available from: https://doi.org/10.1016/j.ijhydene.2019.09.096.

Table 2: Values of r_3, r_4, FWHM(r_3), and FWHM(r_4) estimated from the hole radius distributions

Samples	r_3 (nm) Distribution	r_3 (nm) TE	r_4 (nm) Distribution	r_4 (nm) TE	FWHM(r_3) (nm) Distribution	FWHM(r_4) (nm) Distribution
Without source correction						
Original ETFE	0.246	0.248	0.399	0.399	0.048	0.012
Grafted-ETFE 106%	0.257	0.258	0.356	0.356	0.036	0.013
ETFE-PEM 106%	0.177	0.178	0.322	0.323	0.035	0.009
With source correction						
Original ETFE	0.266	0.265	0.401	0.402	0.054	0.015
Grafted-ETFE 106%	0.257	0.258	0.356	0.356	0.036	0.013
ETFE-PEM 106%	0.204	0.206	0.323	0.323	0.047	0.007

Table 3: Values of V_3, V_4, FWHM (V_3), and FWHM (V_4) estimated from the hole volume distributions

Samples	V_3 (nm^3) Distribution	V_3 (nm^3) TE	V_4 (nm^3) Distribution	V_4 (nm^3) TE	FWHM(V_3) (nm^3) Distribution	Distribution FWHM(V_4) (nm^3)
Without source correction						
Original ETFE	0.060	0.064	0.266	0.266	0.034	0.023
Grafted-ETFE 106%	0.070	0.072	0.189	0.190	0.030	0.021
ETFE-PEM 106%	0.022	0.024	0.140	0.141	0.014	0.012
With source correction						
Original ETFE	0.078	0.078	0.271	0.271	0.046	0.031
Grafted-ETFE 106%	0.070	0.072	0.189	0.190	0.030	0.021
ETFE-PEM 106%	0.034	0.037	0.141	0.141	0.024	0.009

4. Ke Y, Yuan W, Zhou F, Guo W, Li J, Zhuang Z, et al. A critical review on surface-pattern engineering of nafion membrane for fuel cell applications. Renew Sustain Energy Rev. 2021;145(July 2020):110860;Available from: https://doi.org/10.1016/j.rser.2021.110860.
5. Liu F, Yi B, Xing D, Yu J, Zhang H. Nafion/PTFE composite membranes for fuel cell applications. J Memb Sci. 2003;212(1-2):213-23;Available from: https://doi.org/10.1016/S0376-7388(02)00503-3.
6. Tap TD, Nguyen LL, Hasegawa S, Sawada S ichi, Luan LQ, Maekawa Y. Internal and interfacial structure analysis of graft-type fluorinated polymer electrolyte membranes by small-angle X-ray scattering in the high-q range. J Appl Polym Sci. 2020;137(35);Available from: https://doi.org/10.1002/app.49029.
7. Hao LH, Hieu DTT, Long TH, Hoa D Van, Danh TT, Man T Van, et al. Investigation of the Lamellar Grains of Graft-type Polymer Electrolyte Membranes for Hydrogen Fuel Cell Application using Ultrasmall-angle X-ray Scattering. VNU J Sci Nat Sci Technol. 2021;1-9;Available from: https://doi.org/10.25073/2588-1140/vnunst.5216.
8. Dinh TTH, Lam HH, Tran TD, Le QL, Tran VM, Huynh TP, et al. Investigation of the water states of poly(styrene sulfonic acid) grafted poly(ethylene-co-tetrafluoroethylene) copolymer using FT-IR analysis. Minist Sci Technol Vietnam. 2022;64(2):3-9;Available from: https://doi.org/10.31276/VJSTE.64(2).03-09.
9. Hieu DTT, Hao LH, Long TH, Van Tien V, Cuong NT, Van Man T, et al. Investigation of chemical degradation and water states in the graft-type polymer electrolyte membranes. Polym Eng Sci. 2022;62(9):2757-68;Available from: https://doi.org/10.1002/pen.26059.
10. Tao SJ. Positronium annihilation in molecular substances. J Chem Phys. 1972;56(11):5499-510;Available from: https://doi.org/10.1063/1.1677067.
11. Eldrup M, Lightbody D, Sherwood JN. The temperature dependence of positron lifetimes in solid pivalic acid. Chem Phys. 1981;63(1-2):51-8;Available from: https://doi.org/10.1016/0301-0104(81)80307-2.
12. Tap TD, Long TH, Hieu DTT, Hao LH, Phuong HT, Luan LQ, et al. Positron annihilation lifetime study of subnano level free volume features of grafted polymer electrolyte membranes for hydrogen fuel cell applications. Polym Adv Technol. 2022;33(9):2952-65;Available from: https://doi.org/10.1002/pat.5761.
13. Long TH, Hieu DTT, Hao LH, Cuong NT, Loan TTH, Van Man T, et al. Positron annihilation lifetime spectroscopic analysis of Nafion and graft-type polymer electrolyte membranes for fuel cell application. Polym Eng Sci. 2022;62(12):4005-17;Available

from: https://doi.org/10.1002/pen.26162.

14. Sawada S ichi, Yabuuchi A, Maekawa M, Kawasuso A, Maekawa Y. Location and size of nanoscale free-volume holes in crosslinked- polytetrafluoroethylene-based graft-type polymer electrolyte membranes determined by positron annihilation lifetime spectroscopy. Radiat Phys Chem. 2013;87:46-52;Available from: http://dx.doi.org/10.1016/j.radphyschem.2013.02.016.
15. Mcguire S, Keeble DJ. Positron lifetimes of polycrystalline metals: A positron source correction study. J Appl Phys. 2013;103504(2006);Available from: https://doi.org/10.1063/1.2384794.
16. Kanda GS, Keeble DJ. Nuclear Instruments and Methods in Physics Research A Positron annihilation lifetime spectroscopy source correction determination : A simulation study. Nucl Inst Methods Phys Res A. 2015;1-6;Available from: http://dx.doi.org/10.1016/j.nima.2015.11.052.
17. Staab TEM, Somieski B. The data treatment influence on the spectra decomposition positron lifetime spectroscopy Part 2 : The effect of source corrections. Nucl Instruments Methods Phys Res Sect A Accel Spectrometers, Detect Assoc Equip. 1996;Available from: https://doi.org/10.1016/0168-9002(96)00585-2.
18. Search H, Journals C, Contact A, Iopscience M, Address IP. Source correction in positron annihilation lifetime spectroscopy. J Phys Condens Matter. 1996;2081;Available from: https://doi.org/10.1088/0953-8984/8/12/020.
19. Trai N, Chi Minh H, Nam Correspondence Tran Duy Tap V, Nam V, Hoang Hao L, Tran Trong Hieu D, et al. Surface features of polymer electrolyte membranes for fuel cell applications: An approach using S2p XPS analysis. Sci Technol Dev J. 2021;24(3):2100-9;Available from: http://stdj.scienceandtechnology.com.vn/index.php/stdj/article/view/2556.
20. Tran TD, Pham HM, Nguyen AH, Luong AT, Luu TA. Study of lamellar structures of graft-type fluorinated proton exchange membranes by small-angle X-ray scattering: preparation procedures and grafting degree dependence for fuel application. Sci Technol Dev J. 2015;18(3):153-61;Available from: https://doi.org/10.32508/stdj.v18i3.831.
21. Jean YC. Positron annihilation spectroscopy for chemical analysis: A novel probe for microstructural analysis of polymers. Microchem J. 1990;42(1):72-102;Available from: https://doi.org/10.1016/0026-265X(90)90027-3.
22. Minor H, Murthy NS. General procedure for evaluating amorphous scattering and crystallinity from X-ray diffraction scans of semicrystalline polymers. Polymer. 1989;31:996-1002;Available from: https://doi.org/10.1016/0032-3861(90)90243-R.
23. Shpotyuk O, Ingram A, Shpotyuk O. Photopolymerization shrinkage in dimethacrylate-based dental restorative composites probed by means of positron annihilation lifetime spectroscopy. Polymer. 2020;196(April):122485;Available from: https://doi.org/10.1016/j.polymer.2020.122485.
24. Kansy J. Microcomputer program for analysis of positron annihilation lifetime spectra. Analysis. 1996;9002(96):235-44;Available from: https://doi.org/10.1016/0168-9002(96)00075-7.
25. Tap TD. Study on the structure of polymer electrolyte membrane using small angle X-ray scattering and positron annihilation spectroscopy. VNUHCM J Nat Sci. 2017;1(6):197-205;Available from: https://doi.org/10.32508/stdjns.v1i6.630.
26. Liu J, Deng Q, Jean YC. Free-Volume Distributions of Polystyrene Probed by Positron Annihilation: Comparison with Free-Volume Theories. Macromolecules. 1993;26(26):7149-55;Available from: https://doi.org/10.1021/ma00078a006.
27. Del Río J, Etxeberria A, López-Rodríguez N, Lizundia E, Sarasua JR. A PALS contribution to the supramolecular structure of poly(l -lactide). Macromolecules. 2010;43(10):4698-707;Available from: https://doi.org/10.1021/ma902247y.
28. Jean YC, Van Horn JD, Hung WS, Lee KR. Correction to Perspective of Positron Annihilation Spectroscopy in Polymers. Macromolecules. 2013;46(20):8392-8392;Available from: https://doi.org/10.1021/ma401309x.